

Advances in Computational Risk Predictions for Complex, Large-Size Structural Engineering Applications

Dr. Dan M. Ghiocel
Ghiocel Predictive Technologies, Inc., 6 South Main, 2nd Floor
Pittsford, New York 14534, USA
Email: dan.ghiocel@ghiocel-tech.com
Http://www.ghiocel-tech.com

Abstract

The paper discusses the key modeling aspects for solving efficiently and accurately complex, large-size computational stochastic mechanics problems. The paper focus is on stochastic response approximation techniques based on stochastic field models.

1.0 Introduction

There are two critical modeling aspects for solving accurately and efficiently complex, large-size computational stochastic mechanics problems:

(i) Accurate *Stochastic Field Approximation* (SFA) models for complex physical system response behaviors given the statistical sample datasets.

They ensure both an accurate global and local stochastic approximation of the system response based on the sample data space decomposition in a reduced-size state (or feature) space. The SFA models can be viewed as statistics-based reduced-order models (ROM) in sample data space (the constituent elements are local or conditional data densities computed for partially overlapping stochastic partitions in data space).

(ii) Fast *Physics-based Stochastic Simulation* (PSS) models given the physics of the problem (partial differential equation with computed solution via the FE code) and the system stochastic parameters and inputs.

The PSS models are based on the original physical space decomposition in reduced-size subspaces (i) by projecting the solution in a subspace and/or (ii) by optimally partitioning or decomposing the physical domain in *soft* subdomains – these *soft* subdomains can be slightly-overlapping or highly-overlapping.

The paper addresses in a relative detail the first modeling aspect. The reader is also suggested to see an earlier paper of the author (Ghiocel, 2001). The second modeling aspect related to the development of the PSS models is not discussed in herein. Some

information on this aspect is provided elsewhere (Ghiocel, 2004).

Typically, the term *stochastic process* describes a dynamic random phenomenon, while the term *stochastic field* describes a random spatial variation. In the context of continuum mechanics problems, random spatial variations are represented by stochastic surfaces.

A space-time stochastic process is a stochastic function having the time and the space as independent arguments. The term space-time stochastic process is synonym to the term time-varying stochastic field. More generally, a stochastic function is the output of a complex physical stochastic system. Since in continuum mechanics a stochastic response is described by a stochastic surface in input space (for selected ranges of variability), the *stochastic field* term is a more appropriate term for engineering practice. The stochastic field term fits well with stochastic boundary value problems. Only the term of stochastic field is used hereafter.

A stochastic field can be homogeneous or non-homogeneous, isotropic or anisotropic depending if its statistics are invariant or variant to the axis translation and, respectively, invariant or variant to the axis rotation in the physical parameter space.

From a theoretical point of view, a multivariate stochastic field is completely defined by its input-output joint probability density function (JPDF).

2.0 Second-Order Stochastic Field Models

In this section we discuss the covariance-based stochastic field approximation models. Basically, there are two competing stochastic approximation techniques using the covariance kernel factorization: (i) the Choleski decomposition technique and (ii) the Karhunen-Loeve (KL) expansion. They can be employed to simulate both static and dynamic stochastic responses. A notable property of these two stochastic field approximation techniques is that they can handle both real-valued and complex-valued covariance kernels. For simulating space-time processes (or time-varying stochastic fields), the two covariance-based techniques can be employed either in the time-space domain by decomposing the cross-covariance kernel or in the complex frequency-wavelength domain by decomposing the complex cross-spectral density kernel. For real-valued covariance kernels, the application of the KL expansion technique is equivalent to the application of the Proper Orthogonal Decomposition (POD expansion) and Principal Component Analysis (PCA expansion) techniques (Ghiocel, 2004).

More generally, the Choleski decomposition and the KL expansion can be applied to any arbitrary square-integrable, complex-valued stochastic field, $u(\mathbf{x}, \theta)$. Since the covariance kernel of the complex-valued stochastic field $\text{Cov}[u(\mathbf{x}, \theta), u(\mathbf{x}', \theta)]$ is a Hermitian kernel, it can be factorized using either Choleski or KL decomposition. An important practicality aspect of the above covariance-based simulation techniques is that they can be easily applied in conjunction with the inverse marginal probability transformation to simulate non-Gaussian (translation) stochastic fields, either static or dynamic. If the KL expansion is used, the covariance function is expanded in the following eigenseries:

$$\text{Cov}[u(\mathbf{x}, \theta), u(\mathbf{x}', \theta)] = \sum_{n=0}^{\infty} \lambda_n \Phi_n(\mathbf{x}) \Phi_n^*(\mathbf{x}') \quad (1)$$

where λ_n and $\Phi_n(\mathbf{x})$ are the eigenvalue and the eigenvector of the covariance kernel computed by solving the integral equation:

$$\int \text{Cov}[u(\mathbf{x}, \theta), u(\mathbf{x}', \theta)] \Phi_n(\mathbf{x}) d\mathbf{x} = \lambda_n \Phi_n(\mathbf{x}') \quad (2)$$

As a result of covariance function being Hermitian, all its eigenvalues are real and the associated complex eigenfunctions that correspond to distinct eigenvalues are mutually orthogonal. Thus, they form a complete set spanning the stochastic space that contains the field u . It can be shown that if this

deterministic function set is used to represent the stochastic field, then the stochastic coefficients used in the expansion are also mutually orthogonal (uncorrelated in statistical sense).

The KL series expansion has the general form

$$u(\mathbf{x}, \theta) = \sum_{i=0}^n \sqrt{\lambda_i} \Phi_i(\mathbf{x}) z_i(\theta) \quad (3)$$

where set $\{z_i\}$ is the set of uncorrelated random variables that are computed by solving the stochastic integral:

$$z_i(\theta) = \frac{1}{\sqrt{\lambda_i}} \int_D \Phi_n(\theta) u(\mathbf{x}, \theta) d\mathbf{x} \quad (4)$$

The KL expansion is an optimal spectral representation with respect to the second-order statistics of the stochastic field. For many engineering applications on continuum mechanics, the KL expansion is fast mean-square convergent, i.e. only few expansion terms are needed to be included. This fast convergence is a key advantage of the KL expansion over the Choleski decomposition that makes the KL expansion (or POD, PCA) more attractive in engineering practice. This indicates that the transformed stochastic space obtained using the KL expansion has typically a highly reduced dimensionality when compared with the original stochastic space. In contrast, the Choleski decomposition preserves the original stochastic space dimensionality. For this reason, the KL expansion (or POD, PCA) has considered by some researchers to be a *stochastic reduced-order model* for representing complex spatial stochastic patterns.

The KL expansion, in addition to space dimensionality reduction, also provides great insights on the stochastic field structure. The eigenvectors of the covariance matrix play in stochastic modeling a role similar to the vibration eigenvectors in structural dynamics; complex spatial variation patterns are decomposed in just a few dominant spatial variation *mode shapes*.

Translation Non-Gaussian Fields

From a mathematical point of view, a non-Gaussian stochastic field is completely defined by its JPDF. However, in practice, most often, non-Gaussian fields are defined incompletely by the second-order moments (the mean vector and the covariance matrix) and the marginal probability distributions. This incomplete definition loses all the information on the high-order statistical moments.

It should be noted that translation field model incorporate more information (about marginal PDFs) than a standard second-order stochastic field model that implicitly assumes Gaussian variations.

These partially defined non-Gaussian fields form a special class of non-Gaussian fields that are called translation stochastic fields (Grigoriu, 1995, Ghiocel, 2004). Thus, the translation fields are non-Gaussian fields defined by their second-order moments and their marginal distributions. Although the translation field models are not exact models of non-Gaussian stochastic fields they are of a great practicality. Typically, they capture quite accurately the non-Gaussian variability aspects from marginal PDFs.

The translation fields can be also mapped into Gaussian fields. To define a non-Gaussian (translation) stochastic field y with a given covariance matrix Σ_{yy} and a marginal distribution vector \mathbf{F} , first its Gaussian image field \mathbf{x} with a covariance matrix Σ_{xx} and marginal distribution vector $\Phi(\mathbf{x})$ needs to be determined. Then, the observed non-Gaussian field y is obtained by applying an inverse marginal probability distribution transformation of the non-Gaussian distribution F as follows:

$$\mathbf{y} = \mathbf{F}^{-1}\Phi(\mathbf{x}) = \mathbf{g}(\mathbf{x}) \quad (5)$$

However, for simulating the Gaussian image field we need to define its covariance matrix Σ_{xx} as a transform of the covariance matrix Σ_{yy} of the original non-Gaussian field. Between the elements of the scaled covariance matrix or correlation coefficient matrix of the original non-Gaussian field, ρ_{y_i, y_j} and the elements of the scaled covariance or correlation coefficient of the Gaussian image, ρ_{x_i, x_j} there is the relation (Ghiocel, 2004):

$$\rho_{y_i, y_j} = \frac{1}{\sigma_{y_i} \sigma_{y_j}} \int_{-\infty}^{\infty} \int_{-\infty}^{\infty} [F_i^{-1}\Phi(x_i) - \mu_{y_i}] [F_i^{-1}\Phi(x_j) - \mu_{y_j}] \phi(x_i, x_j) dx_i dx_j \quad (6)$$

$$\phi(x_i, x_j) dx_i dx_j$$

where the bivariate Gaussian PDF is defined by

$$\phi(x_i, x_j) = \frac{1}{2\pi(1-\rho_{x_i, x_j}^2)^{0.5} \sigma_{x_i} \sigma_{x_j}} \exp\left(-\frac{1}{2} \frac{(x_i - \mu_{x_i})^2 / \sigma_{x_i}^2 - 2\rho_{x_i, x_j} (x_i - \mu_{x_i}) / \sigma_{x_i} \sigma_{x_j} + (x_j - \mu_{x_j})^2 / \sigma_{x_j}^2}{(1-\rho_{x_i, x_j}^2)}\right) \quad (7)$$

Using translation fields in conjunction with KL expansion, highly non-Gaussian variations can be accurately modeled.

Gaussian Kriging

A Kriging model is based upon the representation of the output of a system analysis as a stochastic field (Cressie, 1991). Usually, the Kriging approximation model consists of two additive components: 1) a simple linear regression of the data, $\mathbf{f}^T(\mathbf{x}) \boldsymbol{\beta}$, and 2) a stochastic variation model, $z(\mathbf{x})$, of the random deviation vector from the linear model. The mean response, $\bar{y}(\mathbf{x})$, at any feasible location, \mathbf{x} , is then computed by

$$\bar{y}(\mathbf{x}) = \mathbf{f}^T(\mathbf{x}) \boldsymbol{\beta} + z(\mathbf{x}). \quad (8)$$

The first part of the model is a linear regression of the observations using a k -dimensional regressor, $\mathbf{f}(\mathbf{x}) = \{f_1(\mathbf{x}), f_2(\mathbf{x}), \dots, f_k(\mathbf{x})\}^T$ and the optimal regression coefficients, $\boldsymbol{\beta}$. The linear regression model is selected to remove any bias from the observations while minimizing the mean-square error (MSE) in their estimate.

Due to its simplicity and good performance, the Gaussian spatial covariance function was considered. First, the correlation matrix, \mathbf{R} , that has is computed. The covariance function is written in the form:

$$\mathbf{R} = \begin{bmatrix} R(\mathbf{x}_1, \mathbf{x}_1) & R(\mathbf{x}_1, \mathbf{x}_2) & \dots & R(\mathbf{x}_1, \mathbf{x}_n) \\ R(\mathbf{x}_2, \mathbf{x}_1) & R(\mathbf{x}_2, \mathbf{x}_2) & \dots & R(\mathbf{x}_2, \mathbf{x}_n) \\ \vdots & \vdots & \ddots & \vdots \\ R(\mathbf{x}_n, \mathbf{x}_1) & R(\mathbf{x}_n, \mathbf{x}_2) & \dots & R(\mathbf{x}_n, \mathbf{x}_n) \end{bmatrix} \quad (9)$$

The correlation between each observation and any unobserved point defined is

$$\mathbf{r}(\mathbf{x}) = \{R(\mathbf{x}, \mathbf{x}_1), R(\mathbf{x}, \mathbf{x}_2), \dots, R(\mathbf{x}, \mathbf{x}_n)\}^T \quad (10)$$

The optimal Kriging model is defined by the following relations:

$$\mathbf{y}(\mathbf{x}) = \mathbf{f}^T(\mathbf{x}) \boldsymbol{\beta} + \mathbf{r}^T(\mathbf{x}) \mathbf{R}^{-1}(\mathbf{Y} - \mathbf{F} \boldsymbol{\beta}) \quad (11)$$

where $\mathbf{f}(\mathbf{x})$ is a vector of functions of the input, \mathbf{x} , such as a constant or a polynomial function, \mathbf{F} is a matrix of $\mathbf{f}(\mathbf{x})$ evaluated at each input point in the set, \mathbf{x} , and:

$$\boldsymbol{\beta} = (\mathbf{F}^T \mathbf{R}^{-1} \mathbf{F})^{-1} \mathbf{F}^T \mathbf{R}^{-1} \mathbf{Y} \quad (12)$$

Finally, the variance of the response is computed by:

$$\text{Var} [\bar{y}(\mathbf{x})] = \sigma^2 \left[1 - \begin{bmatrix} \mathbf{f}^T(\mathbf{x}) & \mathbf{r}^T(\mathbf{x}) \end{bmatrix} \begin{bmatrix} 0 & \mathbf{F}^T \\ \mathbf{F} & \mathbf{R} \end{bmatrix}^{-1} \begin{bmatrix} \mathbf{f}(\mathbf{x}) \\ \mathbf{r}(\mathbf{x}) \end{bmatrix} \right] \quad (13)$$

3.0 High-Order Stochastic Field Models

The concept of high-order stochastic fields is described pictorially in Figures 1 and 2. A high-order stochastic field model is based on the decomposition

of the JPDP of the joint input-output stochastic vector in elementary, local JPDP models. The resulting stochastic local JPDP expansion is capable of describing in detail very complex-pattern multivariate non-Gaussian stochastic fields. As shown in Figure 1, high-order stochastic field models can be implemented as two-layer stochastic neural-network since they represent two-level hierarchical models. Importantly, these two-layer stochastic nets based on local JPDP basis functions train much faster in comparison with the usual multi-layer preceptor (MLP) neural-networks that use sigmoidal nodal basis functions. Their train efficiency is due to the reduced number of layers, only two, and due to the selection of JPDP basis functions that ensure an efficient data modeling and by this a fast convergence of the overall JPDP expansion. It should be noted that if the correlation structure of local JPDP models is ignored, these local JPDP lose significantly their functionality. If the local correlation structure (clusters' orientation) is neglected, a loss of accuracy is produced as shown in Figure 2. The radial-basis functions, such standard Gaussians, or other isotropic kernels ignore the local directional correlation structures. By this radial-basis function models lose accuracy in local modeling of stochastic response surface. A way to improve their results is to reduce their sizes drastically. This requires increase significantly the stochastic model complexity.

If the local JPDP models are well-separated and assumed to be Gaussians, then overall JPDP is approximated by a piecewise Gaussian solution, i.e. the statistical nonlinear interrelationships are locally linearized. A way to improve the local stochastic surface approximation by improving its smoothing is to use a two-level hierarchical model with highly overlapping local Gaussian models, i.e. the stochastic field is not locally approximated by a Gaussian, although the overlapped local JPDP are still Gaussians, as shown in Figure 3. Figure 4 compares the radial-basis function network (RBFN) model (upper plots) with PPCA expansion model (lower plots) for a complex statistical dataset that describes a complex highly non-Gaussian stochastic variability. The bottom plot shows that the overall JPDP estimations for the two models. It can be noted that local PPCA field expansion model is much more accurate than radial-basis function network model. The local PPCA models can elongate along long the clusters (see right-side plots) in any arbitrary

direction. The radial-basis functions do not have this flexibility. Thus, to model a long cluster a large number of overlapping radial-basis functions is needed. It is obvious that for a given approximation accuracy, the local PPCA expansion needs a much smaller number of local models than the radial-basis function model.

This basic idea of the JPDP decomposition in elementary JPDP is not a new idea, but it is based on the classical Parzen mixture density estimator

$$g(\mathbf{u}) = \int f(\mathbf{u}|\alpha)dp(\alpha) \quad (14)$$

where $p(\alpha)$ is a continuous distribution that plays the role of an occurrence probability weighting function (called mixing proportions in AI language) over the local model space. In a discrete form, the weighting function can be expressed for a number N of local JPDP models by

$$p(\alpha) = \sum_{i=1}^N P(\alpha_i)\delta(\alpha - \alpha_i) \quad (15)$$

in which $\delta(\alpha - \alpha_i)$ is the Kronecker delta operator.

Typically the parameter α_i are assumed or known and the discrete weighting parameters $P(\alpha_i)$ are the unknowns. The overall JPDP of the stochastic model can be computed in the discrete form by

$$g(\mathbf{u}) = \sum_{i=1}^N g(\mathbf{u}|\alpha_i)P(\alpha_i) \quad (16)$$

The parameters α_i can be represented by the statistics of the local JPDP models. If local Gaussians are used, then, the overall JPDP expression can be rewritten in a more specific form:

$$g(\mathbf{u}) = \sum_{i=1}^N f(\mathbf{u}|i, \bar{\mathbf{u}}_i, \Sigma_i)P_i \quad (17)$$

where $\bar{\mathbf{u}}_i, \Sigma_i$ are the mean vector and covariance matrix of the local JPDP model i . Also, we have

$P_i = n_i / N, \sum_{i=1}^N P_i = 1$, and $P_i > 0$, for $i = 1, N$. The

Gaussian assumption for the local JPDP models implies that the stochastic field is described only locally by a second-order stochastic field model. This assumption does not impose restrictions on the complexity of the correlation structure or the non-Gaussianity of the stochastic field that is approximated.

We use two types of high-order stochastic field model implementations:

(i) *Cluster-Based Implementation*: Using a reduced-size set of local JPDP models for which

each local model represents a cluster of points in space (a cluster is defined by group of data points that describes a specific pattern or feature within the dataset).

(ii) *Point-Based Implementation*: Using a larger-size set of highly localized JPDP for which each local JPDP model represents a data point in space.

Two-Level Hierarchical Stochastic Models

The two-hierarchical models are based on the overall JPDP factorization using local JPDP models as follows:

$$f(y, \mathbf{x}) = \sum_{i=1}^n f(y, \mathbf{x}|s_i) p(s_i) \quad (18)$$

where y is the stochastic output, \mathbf{x} is the stochastic input vector and notation f is the notation for the probability densities. The argument s is associated with the local JPDP models. Index i is the number of the local JPDP model in the expansion.

To compute the conditional output PDF we divide the overall JPDP by the input vector JPDP:

$$\begin{aligned} f(y|\mathbf{x}) &= \frac{f(y, \mathbf{x})}{f(\mathbf{x})} = \frac{\sum_{i=1}^n f(y, \mathbf{x}|s_i) p(s_i)}{\sum_{i=1}^n f(\mathbf{x}|s_i) p(s_i)} \\ &= \frac{\sum_{i=1}^n f(y|\mathbf{x}, s_i) f(\mathbf{x}|s_i) p(s_i)}{\sum_{i=1}^n f(\mathbf{x}|s_i) p(s_i)} = \sum_{i=1}^n f_i(y|\mathbf{x}) h_i(\mathbf{x}) \quad (19) \end{aligned}$$

It should be noted that in the above equation, the global basis functions $h_i(\mathbf{x})$ is computed as expansions in terms of the local basis functions $f(\mathbf{x}|s_i)$:

$$h_i(\mathbf{x}) = \frac{f(\mathbf{x}|s_i) p(s_i)}{\sum_{i=1}^n f(\mathbf{x}|s_i) p(s_i)} \quad (20)$$

The conditional-mean response surface is computed by integrating the one-dimensional conditional PDF of the output over the entire stochastic input space:

$$\begin{aligned} E[y|\mathbf{x}] &= \int_{-\infty}^{\infty} y f(y|\mathbf{x}) dy = \frac{\sum_{i=1}^n f(\mathbf{x}|s_i) p(s_i) \int_{-\infty}^{\infty} y f(y|\mathbf{x}, s_i) dy}{\sum_{i=1}^n f(\mathbf{x}|s_i) p(s_i)} \\ &= \sum_{i=1}^n E_i[y|\mathbf{x}] h_i(\mathbf{x}, s_i) = \sum_{i=1}^n \bar{y}_i h_i(\mathbf{x}) \quad (21) \end{aligned}$$

The probability-level output surface can be computed by solving the integral equation

$$\begin{aligned} p &= \int_{-\infty}^{y_p} f(y|\mathbf{x}) dy = \int_{-\infty}^{y_p} \frac{\sum_{i=1}^n f(\mathbf{x}|s_i) f(y|\mathbf{x}, s_i) p(s_i)}{\sum_{i=1}^n f(\mathbf{x}|s_i) p(s_i)} dy = \\ &= \int_{-\infty}^{y_p} \sum_{i=1}^n f_i(y|\mathbf{x}) h_i(\mathbf{x}) dy = \int_{-\infty}^{y_p} \sum_{i=1}^n f_i(y|\mathbf{x}) h_i(\mathbf{x}) dy \quad (22) \end{aligned}$$

or, equivalently, by solving the alternate integral equation

$$p = \int_{-\infty}^{y_p} \frac{f(y, \mathbf{x})}{f(\mathbf{x})} dy = \frac{\int_{-\infty}^{y_p} \sum_{i=1}^n f(y, \mathbf{x}|s_i) p(s_i) dy}{\int_{-\infty}^{\infty} \sum_{i=1}^n f(y, \mathbf{x}|s_i) p(s_i) dy} \quad (23)$$

The above two equivalent equations provides accurate estimates of probability-level response surfaces. They are applicable to any non-Gaussian stochastic response surface approximation problem. The second equation is sometime convenient to use if the local JPDP models of the output-input joint space are already available from a clustering analysis.

It should be also noted that the overall JPDP, the conditional-mean and probability-level response surfaces can be computed using the same local basis functions, $h_i(\mathbf{x})$. This indicates that by using the set of local density functions, $h_i(\mathbf{x})$, we can build a accurate estimator of the overall JPDP, but also a accurate estimator of the conditional-mean surface. This remark is important since it brings a new perspective on the stochastic surface approximation problem; it links conceptually the local density function approaches with the local covariance function approaches. It links the higher-order stochastic field models with the Kriging models.

Three-Level Hierarchical Stochastic Models

In three-level hierarchical models, the local JPDP models are further expanded in a new set of JPDP models:

$$f(y, \mathbf{x}) = \sum_{i=1}^n f(y, \mathbf{x}|s_i) p(s_i, \mathbf{x}) = \sum_{i=1}^n \sum_{j=1}^m f_{i,j}(y, \mathbf{x}) \mu_{i,j} \quad (24)$$

The mixing probability coefficient vector now becomes a mixing partition matrix, whose elements correspond to the conditional probabilities that i will belong to j basis function.

The conditional-mean surface can be computed directly by:

$$E[y|\mathbf{x}] = \bar{y}(\mathbf{x}) = \frac{\sum_{i=1}^n \sum_{j=1}^m E_{i,j}[y|\mathbf{x}] f_{i,j}(\mathbf{x}) \mu_{i,j}}{\sum_{i=1}^n \sum_{j=1}^m f_{i,j}(\mathbf{x}) \mu_{i,j}} \quad (25)$$

Fuzzy Weighted Average Schemes for Approximating Mean-Response

The weighted average scheme for approximating the conditional-mean surface is based on the use of equation 21 in conjunction with a set of fuzzy singletons. Two numerical implementations can be applied. The first implementation is called the fuzzy weighted average constant interpolation (WACI) model (similar in concept with a singleton model in the fuzzy logic theory) that is based on direct application by the equation 21. The second implementation is called fuzzy weighted average linear interpolation (WALI) model (similar in concept with the Tanaka-Sugeno model in fuzzy logic theory) and is based on by a modified equation by defining the cluster center points as a linear function of input \mathbf{x} . The WALI model improves locally the stochastic interpolation quality by including the cluster orientation in the interpolation scheme that is an aspect neglected in the WACI model. It should be noted that WALI model can be applied only to the stochastic field approximations that use local JPDP models with full-covariance matrices (PPCA models).

The WACI model computes the conditional mean-surface by

$$E[y|\mathbf{x}] = \bar{y}(\mathbf{x}) = \frac{\sum_{i=1}^{NC} E[y_i] f(\mathbf{x}|s_i) p(s_i)}{\sum_{i=1}^{NC} f(\mathbf{x}|s_i) p(s_i)} = \frac{\sum_{i=1}^{NC} \bar{y}_i f_i(\mathbf{x}, \mathbf{x}_i) p_i}{\sum_{i=1}^{NC} f_i(\mathbf{x}, \mathbf{x}_i) p_i} \quad (26)$$

The WALI model uses a smoothed estimation based on the cluster orientation (given by the correlation structure of the local JPDP). Instead of using data points y_i uses their linear estimation $y(\mathbf{x}_i) = \mathbf{a}_i^T \mathbf{x}_i + b_i$ determined by least-square regression or by directly using the cluster orientation hyperplane (principal direction of minimum variance).

The WALI modified equation is:

$$E[y|\mathbf{x}] = \bar{y}(\mathbf{x}) = \frac{\sum_{i=1}^{NC} y(\mathbf{x}_i) f_i(\mathbf{x}, \mathbf{x}_i) p_i}{\sum_{i=1}^{NC} f_i(\mathbf{x}, \mathbf{x}_i) p_i} = \frac{\sum_{i=1}^{NC} (\mathbf{a}_i^T \mathbf{x}_i + b_i) f_i(\mathbf{x}, \mathbf{x}_i) p_i}{\sum_{i=1}^{NC} f_i(\mathbf{x}, \mathbf{x}_i) p_i} \quad (27)$$

Stochastic Clustering

Assuming that the local JPDP components are multivariate Gaussians, their analytical expression is given by:

$$f_{\mathbf{x}}(\bar{\mathbf{x}}, \Sigma) = \frac{1}{(2\pi)^{\frac{m}{2}} (\det \Sigma)^{\frac{1}{2}}} \exp\left[-\frac{1}{2}(\mathbf{x} - \bar{\mathbf{x}})^T \Sigma^{-1}(\mathbf{x} - \bar{\mathbf{x}})\right] \quad (28)$$

where $\bar{\mathbf{x}}$ is the mean vector and a Σ is the local component (or cluster) covariance matrix.

For a local component i the stochastic covariance matrix is computed by:

$$\Sigma_i = \frac{\sum_{k=1}^N \mu_{i,k} (\mathbf{x}_k - \bar{\mathbf{x}}_i)(\mathbf{x}_k - \bar{\mathbf{x}}_i)^T}{\sum_{k=1}^N \mu_{i,k}} \quad (29)$$

where the factor $\mu_{i,k}$ that is the *conditional probability* that data point k belongs to local Gaussian model i . It should be noted that in order to completely define a local Gaussian PDF model i , we need to compute the generalized Mahalanobis distance, $D(\mathbf{x}, \mathbf{x}_i)$, using the analytical expression:

$$D(\mathbf{x}, \bar{\mathbf{x}}_i) = (\mathbf{x} - \bar{\mathbf{x}}_i)^T \Sigma_i^{-1} (\mathbf{x} - \bar{\mathbf{x}}_i) \quad (30)$$

For an arbitrary orientation of the local Gaussian JPDP (clusters) covariance matrices are fully filled matrices. The principal directions of the covariance matrix define the zero correlation directions. The local Gaussian (cluster) model is elongated along the direction on minimum variance that is defined by the eigenvector of covariance matrix with the smallest eigenvalue.

Fuzzy Clustering

We also use alternate statistical approaches for describing the local clusters, such as possibilistic-based or fuzzy-based approaches. As an alternate to the stochastic cluster covariance matrix, the fuzzy cluster covariance matrix can be used. The fuzzy cluster covariance \mathbf{F}_i is defined by

$$\mathbf{F}_i = \frac{\sum_{k=1}^N \mu_{i,k}^m (\mathbf{x}_k - \bar{\mathbf{x}}_j)(\mathbf{x}_k - \bar{\mathbf{x}}_j)^T}{\sum_{k=1}^N \mu_{i,k}^m} \quad (31)$$

Usually, the parameter m is equal to 2. The correspondent quantity of the conditional probability μ_{ik} is replaced by its possibility-based or fuzzy-based version called the *partition function* defined by:

$$\text{Possibility-based: } \mu_{ij}(\mathbf{x}_i, \bar{\mathbf{x}}_j) = \frac{1}{1 + D(\mathbf{x}_i, \bar{\mathbf{x}}_j)} \quad (32)$$

$$\text{Fuzzy-based: } \mu_{i,k} = \frac{1}{\sum_{j=1}^{NC} \left(\frac{D(\mathbf{x}_i, \bar{\mathbf{x}}_k)}{D(\mathbf{x}_j, \bar{\mathbf{x}}_k)} \right)^{\frac{1}{m-1}}} \quad (33)$$

In the above equations, the generalized distance $D(\mathbf{x}, \mathbf{x}_i)$ has a modified form of the stochastic version:

$$\text{Possibility-based: } D(\mathbf{x}_i, \bar{\mathbf{x}}_k) = (\mathbf{x}_i - \bar{\mathbf{x}}_k)^2 \quad (34)$$

$$\text{Fuzzy-based: } D(\mathbf{x}_i, \bar{\mathbf{x}}_j) = (\mathbf{x}_i - \bar{\mathbf{x}}_j)^T \mathbf{A}_j (\mathbf{x}_i - \bar{\mathbf{x}}_j) \quad (35)$$

where $\mathbf{A}_j = \text{Det}[\mathbf{F}_j]^{1/p} [\mathbf{F}_j]^{-1}$ and p is the input dimensionality.

Fuzzy-based statistical clustering analysis techniques are FCM, Gustafson-Kessel and Subtractive clustering. These fuzzy clustering analysis techniques are powerful statistical analysis tools for building soft partitions in the sample data space.

4.0 Comparative Results

This section compares results that are obtained using different stochastic field modeling techniques for approximating 2D Nelson surface. A set of 100 uniformly distributed random points were used to test the stochastic approximation models. The Nelson surface was assumed (i) smooth surface without noise, and (ii) rough surface with a 10 percent noise. The result comparison is shown in Figures 5 through 8.

The best performer without and with noise is the three-level hierarchical model. For smooth surface, the popular Gaussian Kriging model is also accurate. However, for noisy surfaces, the Kriging approximation accuracy degrades considerably, thus that the surface approximation is much poorer than for smooth surfaces.

5.0 Large-Size Computational Mechanics Models

For large-size computational mechanics models that cannot fit in a single processor, distributed computer resources are needed. Figure 9 shows a parallel computational stochastic mechanics implementation strategy using multiple SMP computers. Both the sample data space and the physical domain of the problem can be decomposed in parallel data subsets and physical subdomains, respectively, as illustrated in the figure. The computer analyst's preference is to use, as much as possible, the sample space decomposition in independent random samples that can be run in parallel very efficiently. However, if the computational mechanics model is too large to fit in a single processor, then the physical problem domain decomposition is required.

6.0 Concluding Remarks

The paper discusses the application of stochastic field models for approximating complex uncertain responses. The paper also addresses briefly the parallel computer implementation aspects for solving large-size stochastic mechanics problems.

7.0 Selected References

1. Ghiocel, D.M., "Stochastic Simulation Methods for Engineering Predictions", *the Chapter 20 of "Engineering Design Reliability Handbook"*, Eds. Nikolaidis, Ghiocel and Singhal, CRC Press, 2004
2. Ghiocel, D.M., "Stochastic Approximation for High-Complexity Problems", *The 2nd MIT Conference on Fluid and Solid Mechanics*, Boston, MA, June 11-14, 2003
3. Ghiocel, D. M., "Modeling of Complex Stochasticity for Gas Turbine Applications", the ICOSAR'01, Newport Beach, June 18-22, 2001
4. Ghiocel, D.M., "Stochastic Field Models for Aircraft Jet Engines", *Journal of Aerospace Engineering ASCE*, Special Issue on Reliability of Aerospace Structures, Vol. 14, No.4, October, 2001
5. Cressie, J., "Spatial Statistics", *Prentice-Hall, Englewood Cliffs* 1991
6. Grigoriu, M., "Applied Non-Gaussian Processes", *Prentice-Hall, Englewood Cliffs*, 1995

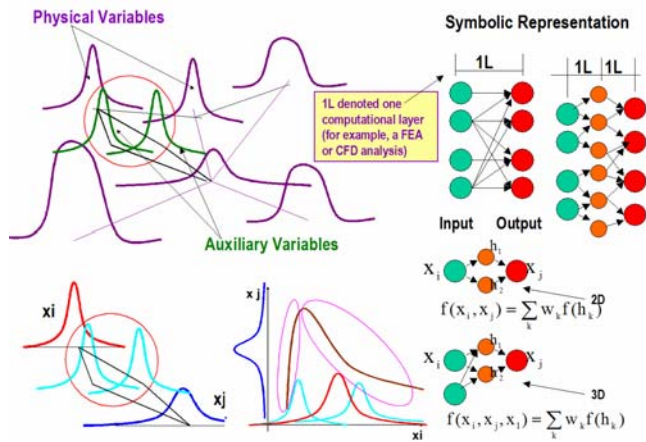


Figure 1. Concept of High-Order Stochastic Fields

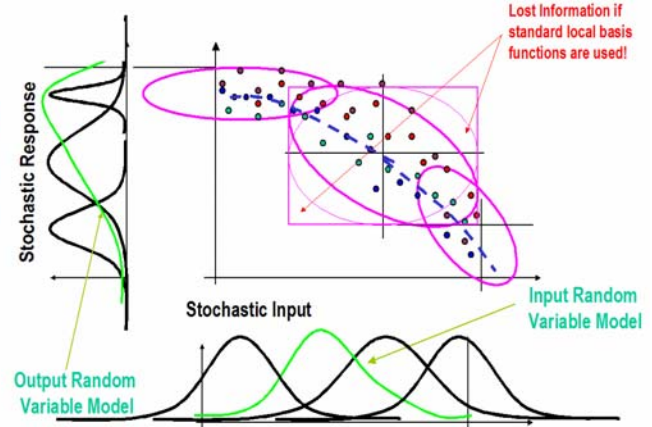


Figure 2. Local JPDP Structure for Bivariate Problem

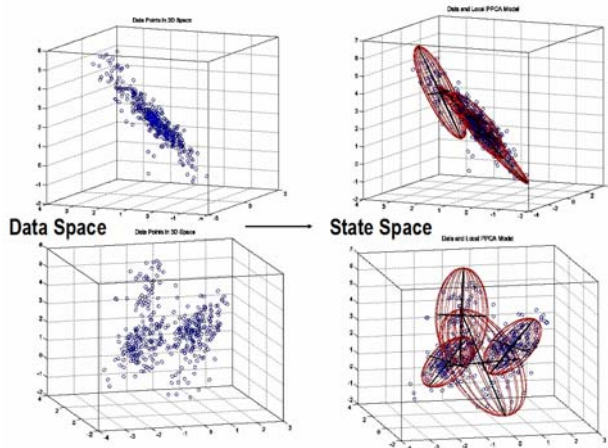


Figure 3. Local Gaussian PPCA Models

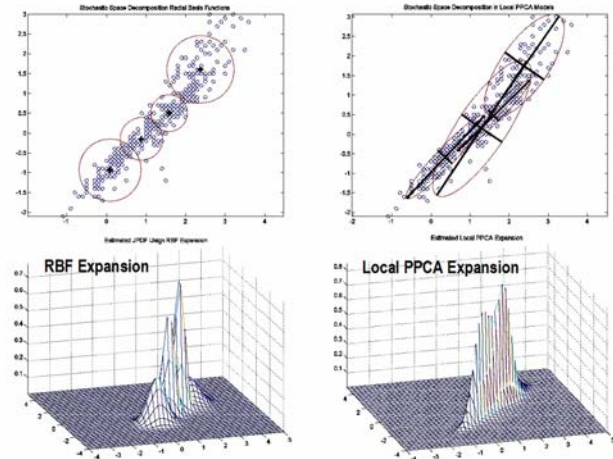
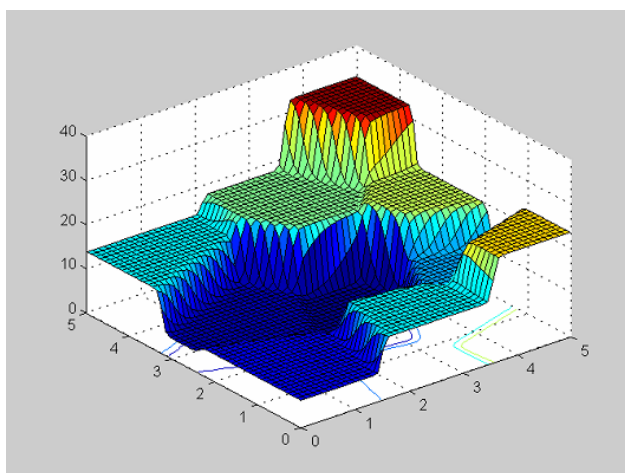
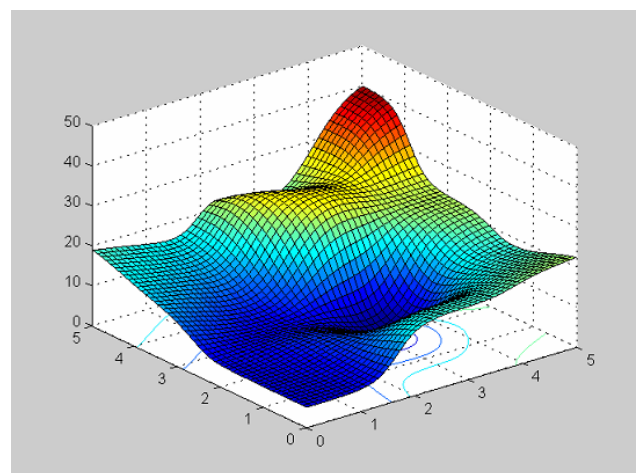


Figure 4. Local RBFN Model vs. PPCA Model

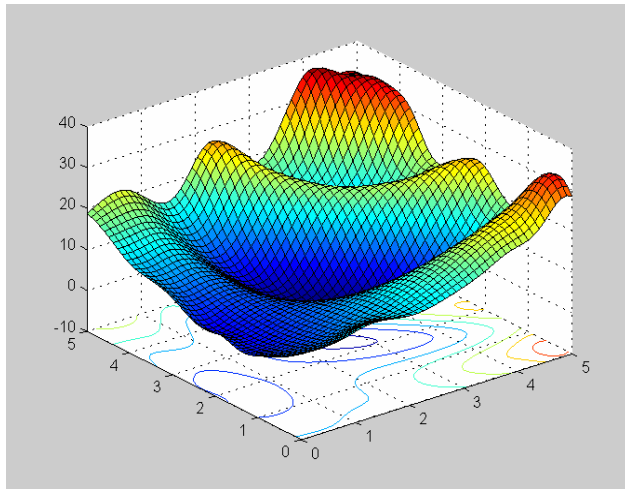


a) Fuzzy Weighted Average Constant Interpolation Using 10 Local Gaussian JPDPs

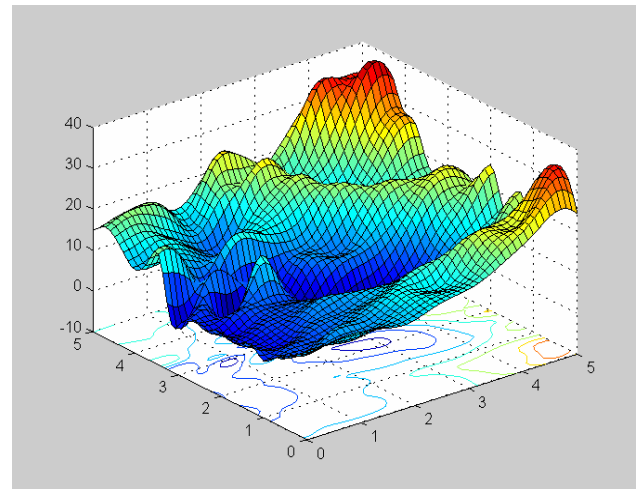


b) Fuzzy Weighted Average Linear Interpolation Using 10 Local Gaussian JPDPs

Figure 5. Comparative Results for Smoothed Nelson Surface Using Fuzzy Weighted Average Techniques for Computing the Mean Response

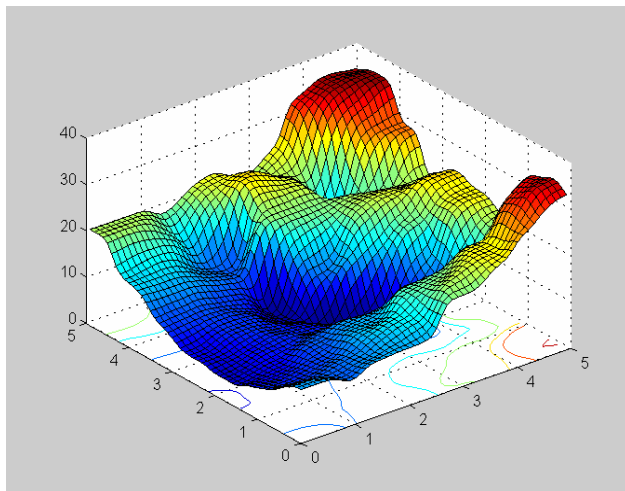


a) 50% Probability-Level Kriging – Smooth

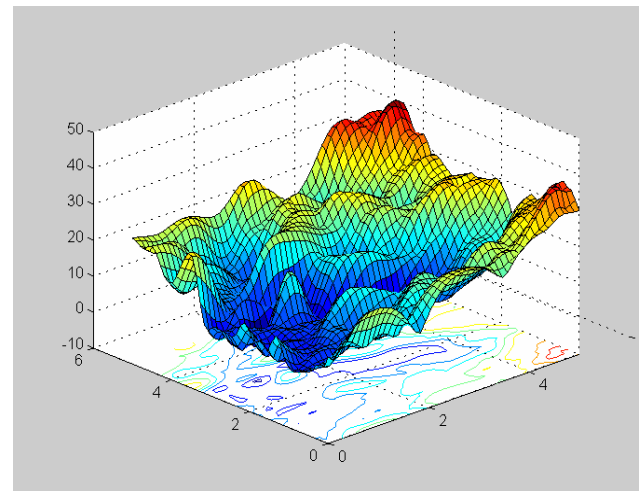


b) 50% Probability-Level Kriging – 10% Noise

Figure 6. Mean Response Surface Approximations Using Kriging Without and With 10% Noise

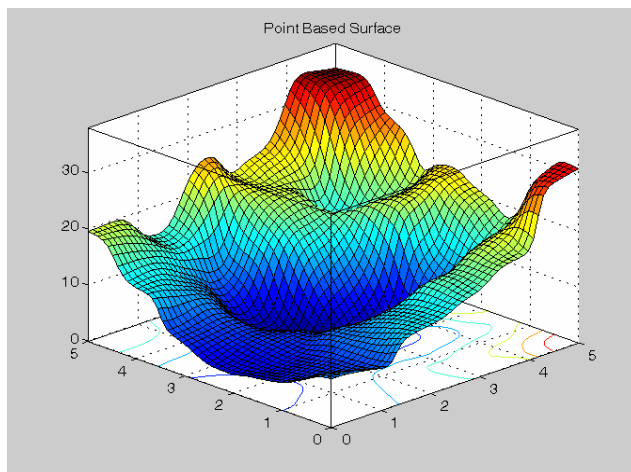


a) 95% Probability-Level Point-Based JPDP

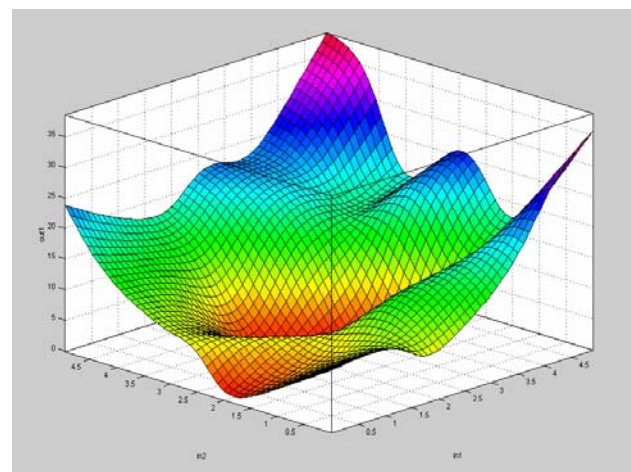


b) 95 % Probability-Level Kriging

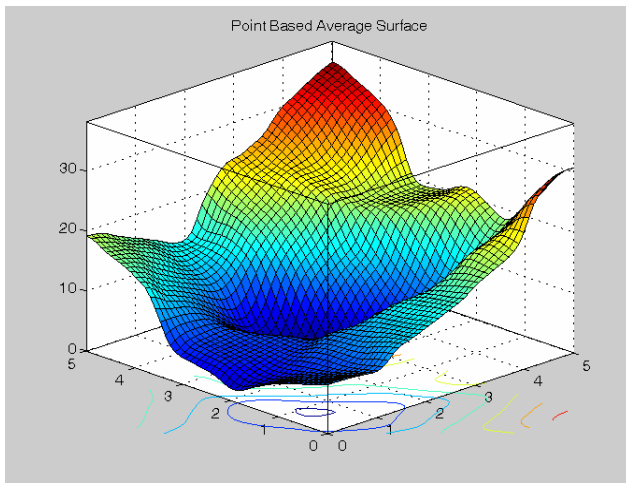
Figure 7. 95% Probability-Level Response Using Point-Based JPDP and Kriging Models With 10% Noise



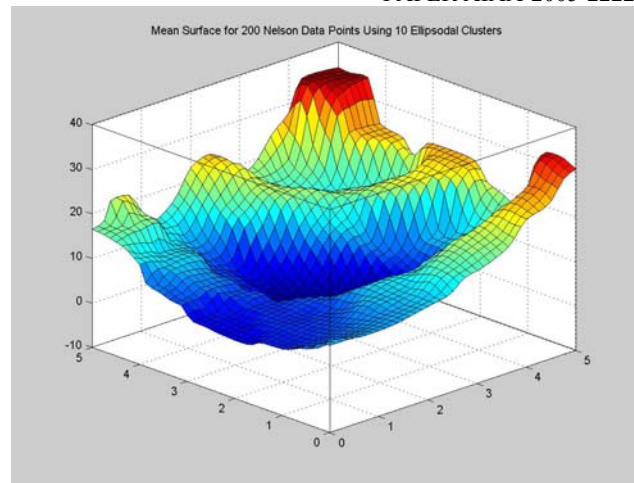
a) 2L HM Using Point-based Local JPDP



b) Adaptive Network-based Fuzzy Inference System (ANFIS) Using 10 Subtractive Clusters



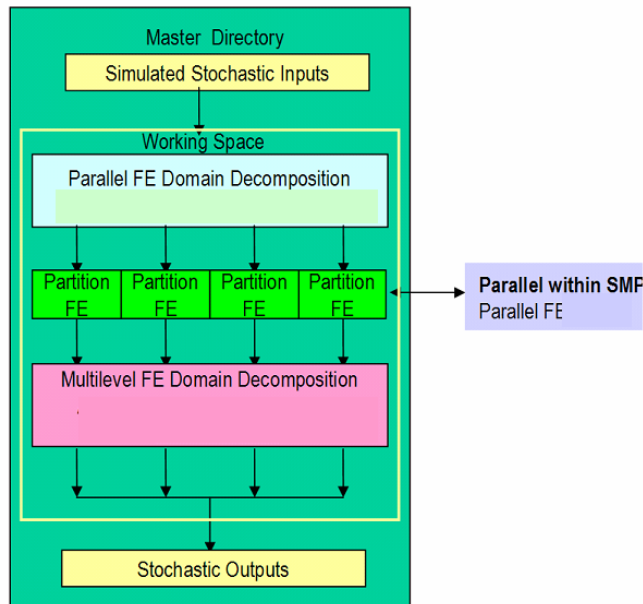
c) MCMC-based Using 10 Local Gaussian JPDF.
Computed by Averaging 8 Simulated Samples



d) 3L HM by Combining Point-based JPDF
with 10 Local Gaussian JPDF

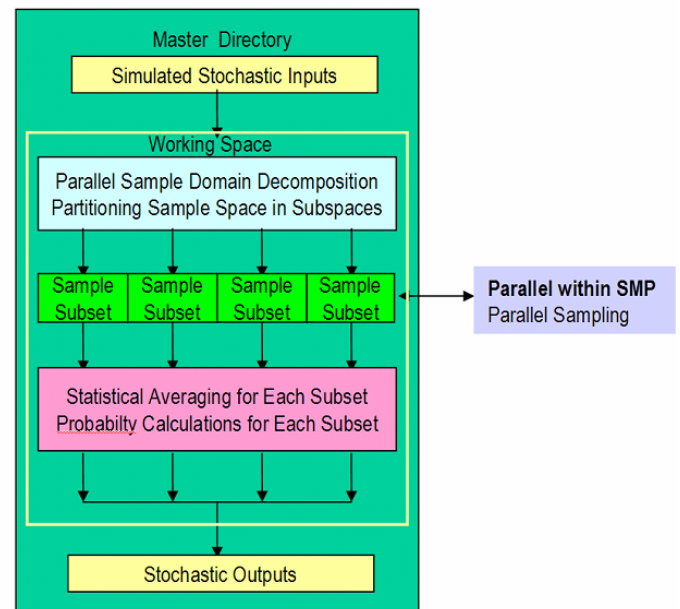
Figure 8. Mean Response Surface Approximations Using Different Stochastic Field Approximation Techniques for Smoothed Nelson Surface

Parallel Decomposition of Physical Space Parallel FEA



Large Models – Few Samples
FE Memory Limited by All SMP Memories

Parallel Decomposition in Stochastic Space Parallel Stochastic Simulation



Reduced Models – Many Samples
FE Memory Limited by Single SMP Memory

Large Models – Many Samples

Figure 9. Combined Parallelization in Computational Stochastic Mechanics Using Distributed Resources